Atmos. Chem. Phys. Discuss., 11, 6555–6599, 2011
www.atmos-chem-phys-discuss.net/11/6555/2011/
doi:10.5194/acpd-11-6555-2011

Atmospheric Chemistry and Physics Discussions

Chemical ozone loss in Arctic and Antarctic polar winter/spring season derived from SCIAMACHY limb measurements 2002–2009

T. Sonkaew[1,2], C. von Savigny[1], K.-U. Eichmann[1], M. Weber[1], A. Rozanov[1], H. Bovensmann[1], and J. P. Burrows[1]

[1]Institute of Environmental Physics, University of Bremen, Otto-Hahn-Allee 1, 28359 Bremen, Germany
[2]Science Faculty, Lampang Rajabhat University, 119 Lampang-Maeta Rd., Lampang, 52100, Thailand

Received: 24 January 2011 – Accepted: 28 January 2011 – Published: 23 February 2011

Correspondence to: T. Sonkaew (thiranan@lpru.ac.th)

Published by Copernicus Publications on behalf of the European Geosciences Union.

Abstract

Stratospheric ozone profiles are retrieved for the period 2002–2009 from SCIAMACHY measurements of limb-scattered solar radiation in the Hartley and Chappuis absorption bands of ozone. This data set is used to determine the chemical ozone loss in both the Arctic and Antarctic polar vortices using the vortex average method. The chemical ozone loss at isentropic levels between 450 K and 600 K is derived from the difference between observed ozone abundances and the ozone modelled considering diabatic cooling, but no chemical ozone loss. The results show chemical ozone losses of up to 20–40% between the beginning of January and the end of March inside the Arctic polar vortex. Strong inter-annual variability of the Arctic ozone loss is observed, with the cold winters 2004/2005 and 2006/2007 showing the largest chemical ozone losses. The ozone mass loss inside the polar vortex is also estimated. In the coldest Arctic winter 2004/2005 the total ozone mass loss is about 30 million tons inside the polar vortex between the 450 K and 600 K isentropic levels from the beginning of January until the end of March.

The Antarctic vortex averaged ozone loss as well as the size of the polar vortex do not vary much from year to year. At the 475 K isentropic level ozone losses of 70–80% between mid-August and mid-November are observed every year inside the vortex, also in the anomalous year 2002. The total ozone mass loss inside the Antarctic polar vortex between the 450 K and 600 K isentropic levels is about 55–75 million tons for the period between mid-August and mid-November.

Comparisons of the vertical variation of ozone loss derived from SCIAMACHY observations with several independent techniques for the Arctic winter 2004/2005 show very good agreement.

ACPD

11, 6555–6599, 2011

1 Introduction

Stratospheric ozone is of great importance, because it protects life on Earth from harmful ultraviolet solar radiation. Stratospheric ozone has been decreasing globally during the second half of the 20th century – due to anthropogenic release of halogen compounds – until about the mid-nineties, when a change of the sign of the ozone trend occurred, particularly in the upper stratospheric region (e.g., Newchurch et al., 2003; Jones et al., 2009; Steinbrecht et al., 2009). The threat by ozone depleting substances was dramatically emphasized with the discovery of the Antarctic ozone hole by Farman et al. (1985), which is now understood as a consequence of different processes, including chlorine activation by heterogeneous chemistry involving polar stratospheric clouds (PSCs) followed by catalytic ozone destruction (e.g., Solomon, 1999). The Antarctic ozone hole is usually associated with the near-total catalytic destruction of ozone in the polar vortex at isentropic levels between about 400 K and 500 K (about 15–20 km altitude) (e.g., Hoppel et al., 2003; Solomon et al., 2005, 2007). Substantial ozone losses in the Arctic polar vortex are also possible during cold winters. Several studies quantified the chemical ozone loss in the Arctic polar vortex using a variety of techniques and instruments (e.g., Chipperfield et al., 1996; Goutail et al., 1997, 2005; Deniel et al., 1998; Becker et al., 2000; Guirlet et al., 2000; Eichmann et al., 2002; Rex et al., 1999, 2002, 2003; Grooß and Müller, 2003). The methods employed to quantify the chemical ozone loss have been divided by Singleton et al. (2005) into four techniques, i.e., (1) the match technique, (2) tracer correlation, (3) passive subtraction and (4) vortex average descent techniques, with each method having different weaknesses. Harris et al. (2002) and Singleton et al. (2005) have compared the chemical ozone losses derived using different techniques, finding generally good agreement.

This paper deals with the determination of polar chemical ozone loss using SCIAMACHY ozone profile measurements in both hemispheres employing the vortex average method (e.g., Knudsen et al., 1998; EU, 2001; Eichmann et al., 2002). The chemical ozone loss at a given isentropic surface is determined from the observed

ACPD
11, 6555–6599, 2011

vortex-averaged ozone abundances correcting for the vertical advection of ozone into and out of this surface.

At high latitudes during winter, solar heating is nearly absent and infrared cooling due to stratospheric water vapor and carbon dioxide dominate (e.g., Siskind et al., 1998; Jucks and Salawitch, 2000). Diabatic descent of ozone-rich air into the lower polar stratosphere occurs during winter. This descent is mostly driven by the Brewer-Dobson (BD) circulation (e.g., Dobson et al., 1930; Brewer, 1949; Haynes et al., 1991; Holton et al., 1995; Rosenlof, 1995; Weber et al., 2003) and has to be corrected for when estimating the chemical ozone loss in the polar vortex.

The two hemispheres exhibit significant differences in terms of the dynamical situation of the polar winter stratosphere and the observed chemical ozone losses inside the vortices. Depletion of ozone in the Arctic lower stratosphere during winter and spring has been detected in some winters when the lower stratosphere was very cold and a stable vortex prevailed for extended periods. The influence of several warmings typically leads to perturbation and final break-up of the Arctic polar vortex by mid-April at the latest. The Antarctic lower stratosphere during winter is characterized by lower temperatures and a generally more stable polar vortex compared to the Arctic polar winter (e.g., Solomon, 1999).

In this paper, we apply the vortex average method to SCIAMACHY observations of stratospheric ozone profiles between 2002 and 2009 to estimate the chemical ozone loss in the Arctic and Antarctic polar vortices. The paper is structured as follows. The SCIAMACHY instrument, whose observations are employed in this study, is briefly described in Sect. 2. A summary of the novel ozone profile retrieval using the SCIATRAN radiative transfer model and the detection of PSCs from SCIAMACHY limb-scatter observations are also provided in this section. Section 3 discusses the determination of the polar vortex boundaries in both hemispheres during winter/spring. The inferred lower stratospheric chemical ozone losses in both hemispheres between 2002 and 2009 are presented and discussed in Sect. 4.

ACPD
11, 6555–6599, 2011

Section 5 deals with comparisons of the vertical variation of chemical ozone loss from SCIAMACHY limb-scatter observations with other instruments for the Arctic winter 2004/2005. The relationship of chemical ozone loss, the occurrence PSCs and the quasi-biannual oscillation (QBO) is discussed in Sect. 6. Conclusions are presented in the last section.

2 The SCIAMACHY instrument and data products

The Scanning Imaging Absorption SpectroMeter for Atmospheric CHartographY (SCIAMACHY) onboard the European environmental Satellite Envisat was launched in March 2002. Envisat is in a near-polar sun-synchronous orbit at 800 km mean altitude and has a 10:00 a.m. local time descending node. Envisat completes about 14.6 orbits per day and achieves full coverage of the sunlit part of the earth in 6 days. SCIAMACHY is an 8-channel absorption spectrometer covering the UV/visible/SWIR spectral range between 214 nm and 2386 nm with a spectral resolution varying between 0.24 nm and 1.48 nm. SCIAMACHY measures scattered and reflected solar radiation in limb and nadir viewing geometries as well as transmitted solar or lunar radiation in occultation mode. In limb viewing geometry the SCIAMACHY instrument scans vertically from the surface up to the top of the atmosphere (about 100 km tangent height) in elevation steps of about 3.3 km. The vertical resolution of the vertical ozone profiles is about 4.5 km. This study employs the SCIAMACHY limb-scatter observations only. Further information on the SCIAMACHY instrument and the mission goals can be found in Bovensmann et al. (1999). In this study we used the ozone profiles and the PSC data products retrieved from SCIAMACHY limb-scatter observations to investigate the polar chemical ozone loss.

ACPD
11, 6555–6599, 2011

2.1 Ozone profile retrievals from SCIAMACHY limb-scatter measurements

In this study we use the new version 2.0 ozone profile data product retrieved from SCIAMACHY limb-scatter measurements at IUP Bremen. A detailed description of the retrieval method was recently provided in Sonkaew et al. (2009). The retrieval is an extension of the method applied by von Savigny et al. (2005a) and combines spectral information from the Hartley, Huggins and Chappuis absorption bands of ozone allowing the retrieval of vertical ozone profiles from the lower stratosphere up to the mesosphere (15–65 km) and is based on the software package SCIATRAN 2.2 (Rozanov et al., 2005; Rozanov, 2008). Spectral information in the Hartley and Huggins bands of ozone is measured in SCIAMACHY channels 1 and 2, ranging from 214 nm to 314 nm, and from 309 nm to 404 nm, respectively. The Chappuis bands are covered by channels 3 and 4 ranging from 394 nm to 620 nm and from 604 nm to 805 nm, respectively. SCIAMACHY Level 1 version 6.03 data is used as a basis for the analysis in this study including the most recent tangent height correction scheme. The Stratozone 2.0 data product provides the vertical variation of ozone concentration (in molecules cm^{-3}) on a regular 1 km altitude grid. This data set has also been used in combination with other stratospheric ozone time series for the ozone trend studies recently published by Steinbrecht et al. (2009) and Jones et al. (2009).

For further processing, the ozone concentrations were converted to ozone mixing ratios using pressure and temperature profiles from the UKMO stratospheric analysis data set (Swinbank and O'Neill, 1994) for the time and location of each SCIAMACHY limb measurement, followed by an interpolation onto a potential temperature (θ) grid.

2.2 Detection of polar stratospheric clouds

Polar stratospheric clouds (PSCs) are also detected using SCIAMACHY limb-scatter observations with a colour-index approach employing two weakly absorbing wavelengths in the near IR (750 nm and 1090 nm) as described in von Savigny et al. (2005b). PSC results will be presented as PSC occurrence rate, which is a

ACPD
11, 6555–6599, 2011

dimensionless quantity and is defined as the ratio of the number of observations with PSC detections and the total number of SCIAMACHY limb measurements – in a given latitude/longitude bin. As demonstrated in von Savigny et al. (2005b) the detections are robust with very few PSC detections at temperatures exceeding 200 K. Unfortunately, H_2SO_4 and HNO_3 have no spectral signatures in the spectral range covered by SCIAMACHY. Therefore, the distinction of different PSC types (in particular the distinction between type Ia and Ib) is not possible. The possibility to identify type II PSCs exploiting the H_2O ice absorption feature in the near-IR is currently investigated.

3 Vortex position

The extent of the polar vortex can be determined using the modified potential vorticity (PV). Following Lait (1994) the modified potential vorticity (MPV) is defined by

$$\mathrm{MPV} = \mathrm{PV}\left(\frac{\theta}{475\,\mathrm{K}}\right)^{-\frac{9}{2}} \quad (1)$$

with θ being the potential temperature and modified potential vorticity unit, $1\,\mathrm{MPVU} = 1 \times 10^{-6}\,\mathrm{m^2\,s^{-1}\,K\,kg^{-1}}$. The vortex boundary is defined by the maximum in the PV gradient and nearly coincides with the region of maximum wind speed and is typically in the range of 35–40 MPVU (Nash et al., 1996; Eichmann et al., 2002). In this study, air masses with absolute MPV values exceeding 38 MPVU are considered to be inside the vortex for both hemispheres. We calculated potential vorticity and modified potential vorticity at isentropic levels between 450 K and 600 K (in steps of 25 K) using pressure, temperature, zonal and meridional wind profiles taken from UKMO assimilated stratospheric data. These isentropic levels correspond to altitudes of about 16–22.5 km.

In general, the two hemispheres exhibit significant differences in terms of stratospheric dynamics. The polar vortex over the Arctic region has been sampled by SCIAMACHY in the cold winters where the lower stratosphere was very cold and a stable

ACPD
11, 6555–6599, 2011

vortex prevailed from November to March. By mid-April the influence of several warmings typically leads to severe perturbations and the break-up of the Arctic vortex. The Antarctic vortex in comparison is characterized by a longer duration, larger extent, and higher stability. This is because the Rossby wave activity – driven by land-sea contrasts and topography – is generally stronger and more variable in the Northern Hemisphere than in the Southern Hemisphere (e.g., Holton and Alexander, 2000).

Figure 1 shows the daily and zonal mean modified potential vorticity values averaged over 5° latitude bins in the Arctic stratosphere region sampled at the geolocations of SCIAMACHY observations and at the 475 K isentropic level from October to April of the winters 2002/2003 to 2008/2009. SCIAMACHY typically starts sampling the Arctic polar vortex in late December/early January, when the vortex becomes illuminated by the sun and limb-scatter observations are possible again.

A strong polar vortex did not form in every year as can be clearly seen in Fig. 1. The colder winters 2002/2003, 2004/2005, 2006/2007, and 2007/2008 show relatively large averaged modified potential vorticity values compared to the warmer winters 2003/2004 and 2005/2006. The appearance of high potential vorticity is in good correspondence with stratospheric temperature data, e.g., from Sounding of the Atmosphere using Broadband Emission Radiometry (SABER) instrument observations (Remsberg et al., 2008; Fussen and López-Puertas, 2009), and the National Centers for Environmental Prediction (NCEP) (CPC, 2009). They showed that long periods of low temperature, less than 200 K, in the lower stratosphere, around 18–20 km, were observed during northern winters 2002/2003, 2004/2005, 2006/2007, and 2007/2008. In 2005/2006 and 2008/2009 major stratospheric sudden warmings (SSWs) occurred. These events correspond to the sudden drop in enhanced potential vorticity occurring in the first half of February in 2006 and 2009. The major SSWs penetrated from the middle stratosphere to the lower stratosphere and severely disturbed the polar vortex as reported by, e.g., Manney et al. (2005a, 2009) and Sathishkumar et al. (2009).

Figure 2 shows the daily and zonal mean modified potential vorticity values in the Antarctic stratosphere at the 475 K isentropic level and sampled at geolocations of

ACPD
11, 6555–6599, 2011

SCIAMACHY observations for the period May to December, 2002–2008. The figure shows that the polar vortex is essentially limited to latitudes poleward 50°–55° S. Obviously, there is much less inter-annual variability of the southern polar winter stratosphere as compared to the Northern Hemisphere. Note, that SCIAMACHY cannot observe southern high latitudes during June to July – because solar radiation is required for the observations – thus the initial formation of the polar vortex does not appear in Fig. 2. It is worth to be noted here that a weak polar vortex can be clearly seen in Fig. 2 during spring 2002. This year was characterized by a very unusual phenomenon in the Southern Hemisphere, i.e., the first observed mid-winter major stratospheric warming in the Southern Hemisphere (e.g., Baldwin et al., 2003; Hoppel et al., 2003; Kushner and Polvani, 2004; Bodeker et al., 2005; IPCC/TEAP, 2005; Newman and Nash, 2005; Ricaud et al., 2005; Konopka et al., 2005; Manney et al., 2005b; von Savigny et al., 2005a). This major warming resulted from anomalously strong planetary wave activity in the Southern Hemisphere which caused a split of the polar vortex into two parts associated with a splitting of the ozone hole. The overall size of the ozone hole in late September 2002 was only about 10% of its usual value (Stolarski et al., 2005).

From Figs. 1 and 2 it is evident that a sufficient sampling of the polar vortex is provided by SCIAMACHY. This means that the vortex average method can be applied to SCIAMACHY to derive polar ozone losses.

4 Determination of chemical ozone loss with the vortex average method

Using the vortex average approach, we determine the mean ozone mixing ratios in the 450 K–600 K isentropic level range taking an average over all SCIAMACHY observations inside the polar vortex on a given day. At a given isentropic level, the ozone mixing ratio may also change due to diabatic descent (or possibly ascent). Correcting the observed mixing ratios for dynamical changes due to diabatic descent yields the chemical ozone loss. This implies that the approach is based on the assumption, that the vortex air masses are well contained inside the polar vortex, i.e., transport across

ACPD
11, 6555–6599, 2011

the vortex boundary is neglected.

We now briefly explain the algorithms used to determine the chemical ozone loss inside the polar vortices. The algorithm used for calculating the chemical ozone loss is the SODD (SCIAMACHY Ozone and Diabatic Descent) program package which is based on the FUDD (FUrm ozone and Diabatic Descent – where FURM stands for FUll Retrieval Method, Hoogen et al., 1999) that has initially been developed to calculate the chemical ozone loss from GOME (Global Ozone Monitoring Experiment) ozone profile retrievals (Eichmann et al., 2002). In this work, the SODD program package was adapted to SCIAMACHY observations and extended to calculate the chemical ozone loss in the Antarctic polar vortex in addition to the Arctic. The diabatic heating rate (Q) at each isentropic level considered is calculated with the MIDRAD radiative transfer model (Shine, 1991) that uses temperature and pressure profiles taken from the UKMO stratospheric assimilation. MIDRAD is run for conditions at the geolocations of all SCIAMACHY observations on a given day. Information on the short wavelength absorption by ozone and the long wavelength absorption and emission by water vapor and carbon dioxide in the stratosphere are required for the calculation. The CO_2 mixing ratio is assumed to be constant at a value of 378 ppmv and the water vapour profiles are taken from the UARS HALOE climatology (Randel et al., 1998) as in Eichmann et al. (2002). The ozone profiles used in the MIDRAD calculations are from SCIAMACHY observations.

The temporal change in ozone mixing ratio at a certain isentropic level caused by vertical transport is calculated using the following equation (e.g., Braathen et al., 1994):

$$\frac{\partial \mathrm{O_3}^{d}}{\partial t} = -Q\left(\frac{p_0}{p}\right)^{\kappa}\frac{\partial \mathrm{O_3}}{\partial \theta} \tag{2}$$

with $\frac{\partial \mathrm{O_3}}{\partial \theta}$ being the partial derivative of the ozone mixing ratio with respect to potential temperature (θ), p and p_0 are pressure at the considered isentropic level and the surface, respectively, and $\kappa = 2/7$ is the ratio of dry air gas constant and specific heat capacity at constant pressure.

ACPD
11, 6555–6599, 2011

4.1 Arctic chemical ozone loss

Figure 3a shows daily averaged ozone mixing ratios at the 475 K isentropic level derived from SCIAMACHY limb measurements inside the Arctic polar vortex for all available seasons. The standard deviations about the daily vortex-average ozone mixing ratios are shown only for the year 2005. Days with missing data and days where the SCIAMACHY instrument did not sample the vortex have been filled with a spline interpolation. The solid lines show the resulting time series smoothed with a 3-day boxcar function. Because the dynamical situation in the Arctic is much more variable than in the Southern Hemisphere, the reference date for the determination of the accumulated ozone loss inside the vortex was chosen individually for every season as given in Table 1. The start day of the studied period is selected as the first spike in ozone mixing ratio in January of each year. The end day of the studied period was chosen as the last day with observations at locations with MPV values exceeding 38 MPUV in the investigated isentrope range. These choices are arbitrary to a certain extent, and will weakly affect the derived total relative ozone losses, but they do not affect the main conclusions of this study.

The daily changes of ozone mixing ratio due to vertical transport associated with diabatic cooling are determined at each isentropic level. The computed daily ozone change (DOC) rates due to diabatic descent (or ascent) (in ppbv day^{-1}) at the 475 K isentropic level for the Arctic vortex are shown in panel b of Fig. 3. Apparently the daily ozone change rates inside the Arctic vortex vary from year to year. Especially in March of 2005, unusually large dynamically induced ozone changes at the 475 K isentropic level were observed (panel b of Fig. 3). An episode with negative diabatic ozone change values was detected in 2004 (dark blue line). This period corresponds to the unique characteristics of a stratospheric warming (Manney et al., 2005a).

The accumulated diabatic ozone changes were calculated from the beginning of each studied period and are displayed as dashed lines in panel c of Fig. 3 for the Arctic polar vortex. The chemical ozone loss inside the vortex is then determined by

ACPD
11, 6555–6599, 2011

subtracting the observed vortex average ozone mixing ratio from the modelled diabatic ozone change. The resulting chemical ozone loss time series are shown in panel d of Fig. 3. The dotted lines in the same panel represent linear fits to the chemical ozone loss time series. Panel e shows the relative chemical ozone loss in percent relative to the start dates listed in Table 1.

The chemical ozone losses inside the Arctic polar vortex exhibit a strong inter-annual variability. The maximum absolute ozone loss derived for the winters 2002/2003 to 2008/2009 inside the Arctic vortex is about 2 ppmv (corresponding to relative losses of 40%) and occurred in March of the years 2005 and 2007. In March 2008 an absolute loss at the 475 K isentropic level inside the Arctic vortex of about 1 ppmv is retrieved (20–30%), and for spring 2004 and 2006 no indications for significant chemical ozone losses were observed.

The derived daily chemical ozone loss rates for the Arctic polar vortex are summarized in Table 1. The daily ozone loss rates were determined in two different ways: (a) by taking the average loss rate over the periods considered (4th column in Table 1); and (b) from the linear fits shown in panel d of Fig. 3 (6th column in Table 1 for 475 K isentropic level). The results in Table 1 show that the calculated chemical ozone loss rates from the linear fit and from the start-end days of the studied period may differ by several ppbv per day, but they are more or less consistent, especially in terms of their inter-annual differences. The highest chemical ozone loss rate over the Arctic stratospheric region is observed in 2009. However, it occurred only in the short period during the end of January and the first half of February when the lower stratosphere was very cold. At the end of January, a SSW occurred and limited the chemical ozone depletion processes. A SSW event also occurred in early 2006 but it affected the lower stratosphere not as strongly as in 2009. Significant chemical ozone losses over the Arctic region were found in 2005, 2007, 2008 and 2003 with the years being listed in decreasing order in terms of ozone losses.

Figure 4 shows maps of PSC occurrence rates in the Arctic for February of the years 2003 to 2009. Apparently there is a good qualitative agreement of the February PSC

ACPD
11, 6555–6599, 2011

occurrence rates and the cumulative chemical ozone loss inside the Arctic vortex for the corresponding years shown in Fig. 3. The Arctic winters 2004/2005, 2006/2007, and 2007/2008, showing the largest ozone losses also had the largest PSC occurrence rates in February. We also note the apparent alternating behavior of low and high PSC occurrence rates and chemical ozone losses in consecutive years, with low PSC occurrence rates in 2004 and 2006, and higher occurrence rates – compared to the following year – in 2003, 2005, and 2007. This alternating behavior is very likely related to the phase of the quasi-biennial oscillation (QBO) and is further discussed below in Sect. 6.

The chemical ozone losses were also computed at different isentropic levels (450 K–600 K, in 25 K steps) using the vortex average method. The ozone depletion in mixing ratio as a function of time and isentropic levels for the Arctic region is presented as contour plots in Fig. 5. The individual start day of each season is listed in Table 1 and the derived daily chemical ozone loss rates are presented in columns 5 to 11 of Table 1.

The substantial ozone losses in the 2004/2005 and 2006/2007 Arctic winter stratosphere are obvious in Fig. 5. According to the panels of this figure, the peak ozone loss exceeding 1.4 ppmv occurs in March of both years in the lower stratosphere between the 450 K and 525 K isentropic levels. The ozone depletion at these levels involves the chlorine chemistry in the polar vortex (e.g., Dufour et al., 2006; Solomon, 1999), with chlorine being released from both of the reservoir gases HCl and $ClONO_2$. When the sun reappears in spring the catalytic ozone destruction chains begin. The region of maximum ozone depletion gradually descends to lower altitudes over the course of the winter but in late winter/early spring ozone depletion in most cases increases above 575 K. The ozone loss above the 550 K isentropic level can be attributed to catalytic ozone destruction due to NO_x and has been reported in several earlier studies (Grooß and Müller, 2007; Grooß et al., 2005; Konopka et al., 2007). Konopka et al. (2007) suggested that the substantial ozone loss in the upper part of the polar vortex is caused by the horizontal transport of the NO_x from the subtropics rather than the descent of NO_x-rich air masses from the mesosphere.

ACPD
11, 6555–6599, 2011

Indications for significant ozone depletion cannot be detected in the 2003/2004 and 2005/2006 polar vortices in the Arctic region. The data gap in 2006 between the 500 K and 550 K isentropic levels starting in early March is due to the fact that no SCIAMACHY observations are available inside the polar vortex defined by the MPV criterion introduced in Sect. 3.

We now use the derived accumulated chemical ozone loss inside the polar vortex to estimate the ozone mass loss within the polar vortex between the 450 K and 600 K isentropic levels. The spatial extent of the polar vortex for the 450–600 K isentrope range is extracted from the UKMO stratospheric analyses on a daily basis using the vortex criterion introduced in Sect. 3. The ozone mass loss for a certain isentrope range is determined from the polar vortex volume and the derived chemical ozone loss followed by a conversion to mass loss per volume. The total ozone mass loss for the 450 K to 600 K isentrope range is then determined by integration over this isentrope range.

The temporal variation of the Arctic polar vortex volume between the 450 K and 600 K isentropic levels for the period from 1 January to 15 April is shown in the left panel of Fig. 6. The polar vortex size in the Arctic region varies substantially from year to year. The largest polar vortex volume within the 450–600 K isentrope range occurred in 2005 with about 200×10^6 km^3 lasting from the beginning of January until mid-March. The ozone mass loss time series are shown in the right panel of Fig. 6. For the winter 2004/2005 the ozone mass loss reached a maximum value of about 30 million tons and dropped after mid-March, probably due to vortex erosion and enhanced mixing with middle latitude air. For the winters 2006/2007 and 2007/2008 the ozone mass loss reached values of about 10 million tons. It must be mentioned that for the period after mid-March the determined mass losses are less reliable, because air masses from outside the vortex may be mixed into the vortex. For the winters 2003/2004, 2005/2006 and 2008/2009 the ozone mass losses are shown only until the beginning of February, because stratospheric warmings caused a sudden decrease in polar vortex volume, and because of the non-significant chemical ozone losses during these winters.

ACPD
11, 6555–6599, 2011

In Fig. 7 the averaged daily polar vortex volume between the 450 K and 600 K isentropic levels is plotted against the accumulated daily ozone mass loss during the time period as shown in the right panel of Fig. 6 for the Arctic winters 2002/2003 to 2008/2009 (blue circles). The largest ozone mass loss and averaged daily polar vortex volume occurred in winter 2004/2005 with values of about 30 million tons and 180×10^6 km^3, respectively. The low averaged daily polar vortex volumes and the non-significant ozone mass losses that occurred in the short periods for the winters 2003/2004, 2005/2006 and 2008/2009 are shown as open-blue circles in Fig. 7 and are in agreement with the results presented earlier.

4.2 Antarctic chemical ozone loss

The results for the Antarctic polar vortex are presented in Fig. 8 in a similar way as the results for the Arctic vortex shown in Fig. 3. Fig. 8a shows the averaged ozone mixing ratio inside the Antarctic vortex at the 475 K potential temperature level. Panel d of Fig. 8 shows that the ozone loss rates are larger in August and September than in October, when the chemical ozone loss stops. The chemical ozone loss during the 3-month period from 15 August to 15 November reaches 2–3 ppmv or 28–33 ppmv day^{-1} (averaged over the 3-month period) every year as shown in panel d of Fig. 8 and Table 2, respectively. The relative ozone losses are shown in Fig. 8e and amount to about 70–80% at the 475 K level by the end of October.

The seasonally averaged daily chemical ozone loss rates inside the Antarctic polar vortex are summarized in Table 2. The ozone loss rates for 2002–2008 show little interannual variability and are between 26 and 32 ppbv per day. The calculated average ozone loss rate maximizes at about 32 ppbv per day in 2007 for the 475 K level. The ozone loss inside the polar vortex in 2002, as presented in Fig. 8, is essentially the same as in all other years considered. This result differs somewhat from the study of Hoppel et al. (2003), who found the ozone loss in the Antarctic vortex about 20% smaller than for the other years analyzed (1994–2001). It is, however, consistent with the fact that chlorine activation in 2002 as evident from OClO observation by GOME was only slightly lower than in other Antarctic winters (see Fig. 4 in Weber et al., 2003).

ACPD
11, 6555–6599, 2011

PSC maps for the austral winter/spring of the years 2002 to 2008 are shown in Fig. 9. Apart from 2002 the differences in September mean PSC occurrence rates over Antarctica for the different years are rather small. The low PSC occurrence rates in September 2002 are mainly a consequence of the major stratospheric warming leading essentially to the disappearance of PSCs within a few days after 22 September (e.g., von Savigny et al., 2005a).

Figure 10 presents contour plots of the Antarctic ozone loss as a function of time and potential temperature – similar to Fig. 5 for the Northern Hemisphere – for the period 15 August to 15 November of each year.

The chemical ozone loss rates are shown in Table 2. Obviously the Antarctic polar vortex is affected by more severe chemical ozone losses compared to the Arctic vortex and is characterized by a rather small inter-annual variability in chemical ozone loss. As shown in Fig. 10, the maximum absolute ozone loss in terms of mixing ratio occurs near the 500 K isentropic level, but the entire potential temperature range studied is affected by substantial ozone losses, particularly towards the end of the period considered.

Another noteworthy result of the present analysis is the fact, that the relative ozone losses between the 450 K and 500 K isentropic levels do not exceed 80%, while many other studies report ozone losses of more than 90% at these levels (e.g., Hoppel et al., 2003). This apparent discrepancy can be attributed to the more limited vertical resolution of the SCIAMACHY ozone profiles of about 4.5 km (given by the Full Width at Half Maximum (FWHM)) of the averaging kernels).

As for the Arctic region, the polar vortex volume and the ozone mass loss are also estimated for the Antarctic region. The polar vortex volume between the 450 K and 600 K isentropic levels is shown on a daily basis in the left panel of Fig. 11 for the period 15 August to 15 November of each year studied. The volume of the polar vortex is similar for all years with values of around 200–290 $\times 10^6$ km^3 except for 2002 when the sudden stratospheric warming occurred around 22 September leading to a drop of the vortex volume to about 150 $\times 10^6$ km^3. The ozone mass losses are shown in the right panel of Fig. 11 and reach values of about 55–75 million tons at the end of the season

ACPD
11, 6555–6599, 2011

in all years except for 2002, when the values decrease after the end of September. It is worth noting here that the polar vortex was less perturbed at altitudes between 16 and 22 km than at 26 km after 22 September 2002 as presented in von Savigny et al. (2005a). Moreover, the observed ozone losses inside the polar vortex are similar for the 2002 Antarctic season until end of September compared to the other years, as shown in Table 2 and Fig. 10. The polar vortex volume and ozone mass loss inside the polar vortex still remained high after the September 2002 sudden stratospheric warming. The scatter plot in Fig. 7 also shows as red circles the average daily Antarctic polar vortex volume between the 450 K and 600 K isentropic levels as a function of the accumulated ozone mass loss. The averaged daily polar vortex volume is about 180–250 $\times$ 10^6 km^3 and the sum of the daily ozone mass loss is about 55–75 million tons for every year over the study period and again the smallest averaged daily polar vortex size occurred in 2002. We note that the averaged Antarctic polar vortex volume in 2002 is almost equal to that of 2004/2005 for the Arctic polar vortex.

5 Comparison of the chemical Ozone loss derived from SCIAMACHY measurements to independent observations and models

The chemical ozone loss derived from SCIAMACHY limb measurements using the vortex average method in the Arctic stratosphere 2004/2005 is selected for a comparison with other data sources and techniques. This year was chosen, because it was characterized by an unusually large catalytic ozone loss as documented in numerous studies (e.g., Dufour et al., 2006; Grooß and Müller, 2007; Singleton et al., 2007, 2005; Rösevall et al., 2008; Rex et al., 2006). Based on data from Rex et al. (2006) the vertical variation of the chemical ozone loss in terms of mixing ratio versus potential temperature for the time period from 5 January to 25 March 2005 and derived from measurements with different instruments is presented in Fig. 12. The red solid circles show the corresponding ozone loss derived from SCIAMACHY observations using the vortex average technique. Note, that no SCIAMACHY data below the 425 K isentropic

ACPD
11, 6555–6599, 2011

level is presented here, because SCIAMACHY did not sample the vortex below the 425 K level during the first half of January, according to the vortex criterion employed here. The error bars represent standard deviations based on error propagation of the standard deviations of the observed mean vortex ozone and the estimated diabatic ozone change. The light-green, black and orange lines are based on POAM II/III, SAGE III and ozonesonde measurements, respectively. The dark-blue line is taken from Rex et al. (2006) and based on the Match method. The light-blue line was simulated with the Chemical Lagrangian Model of the Stratosphere (CLaMS) and is taken from Grooß and Müller (2007).

Figure 12 shows that the vertical variation of the chemical ozone loss derived from SCIAMACHY ozone profile measurements is in quite good agreement with the other data sources and methods. The exception are the results from the CLaMS model which show lower chemical ozone losses below the 475 K isentropic level. Grooß et al. (2008) have quantified – using CLaMS model simulations for the Arctic winter 2002/2003 – the impact of transport across the vortex edge on the ozone loss estimation. They showed that vortex average ozone loss rates determined with the Match technique were larger than the polar vortex average ozone loss in CLaMS below the 450 K isentropic level. Therefore, one of the reasons for the discrepancy between CLaMS and the other results may be across-vortex transport, as the transport across the vortex edge is ignored in the other techniques, including the vortex average technique applied to the SCIAMACHY data in this study.

Singleton et al. (2007) used the passive subtraction technique to quantify the daily chemical ozone loss using the SLIMCAT model and ozone measurements from the POAM III, SAGE III, EOS MLS, ACE-FTS, and MAESTRO instruments by averaging over the measurement locations inside the vortex during the period from December 2004 to March 2005 in the Arctic stratosphere. All instruments provided consistent results, with a maximum inferred ozone loss of 2–2.3 ppmv at the 450–475 K isentropic level, which is slightly larger than the ozone losses estimated in the present study (see panel d of Fig. 3). Grooß and Müller (2007) used CLaMS model simulations to estimate

ACPD
11, 6555–6599, 2011

the chemical ozone loss in the same year applying the vortex average method. The ozone loss results from Singleton et al. (2007) and Grooß and Müller (2007) exhibit a similar pattern compared to the ozone losses derived from SCIAMACHY limb observations using the vortex average method shown in Fig. 5, i.e., the major ozone loss in the lower stratosphere peaking at about the 450 K–500 K isentropic levels. In addition, there is good correspondence of the chemical ozone loss feature at higher isentropic levels in Fig. 5 (~575–600 K at the end of studied period) with the CLaMS results presented by Grooß and Müller (2007). However, this feature – attributed to NO_x driven catalytic ozone loss – does not appear in the multi-instrument analysis of Singleton et al. (2007).

6 Discussion

Maps of PSC occurrence were already used in the previous section to illustrate the good qualitative correspondence between polar chemical ozone loss and PSC occurrence rate in the Northern Hemisphere. In this section we discuss the relationship in more detail.

Figure 13 shows a scatter plot of the zonally averaged PSC occurrence rate (for the months of February and the 40°–65° N latitude range) and the polar chemical ozone loss at the 475 K isentropic level until 1 April of each year. Note, that 2006 and 2009 (open circles) are not included in the linear fitting, because these winters were characterized by stratospheric sudden warmings and the chemical ozone losses were not determined until 1 April for these years. There is a clear dependence of the derived chemical ozone loss on PSC occurrence rate, which is not surprising. Although the exact relationship between PSC occurrence rate and other related quantities, e.g., PSC volume is difficult to establish, our results qualitatively confirm earlier studies, Rex et al. (e.g., 2006) (their Fig. 3).

In Fig. 14 we show the time series of the Arctic chemical ozone loss at 475 K isentropic level by 1 April of each year (black line), together with the PSC occurrence rate

ACPD
11, 6555–6599, 2011

time series for the months of February and for the 40°–65° N latitude range (red line). Again, the good correspondence is obvious. The letters E and W indicate the easterly/westerly phase of the QBO (e.g., Baldwin et al., 2001). This depiction now suggests a clear dependence of the relative magnitude of both the chemical ozone loss and the PSC occurrence rate on the phase of the QBO. The QBO westerly phase appears to be associated with large PSC occurrence and ozone losses, and the easterly phase with lower PSC occurrence rates. This is consistent with the Holton-Tan mechanism (Holton and Tan, 1980) that related the westerly phase of the QBO with a more stable Arctic and colder vortex, subsequently leading to higher PSC occurrence and larger chemical ozone destruction. According to Labitzke (1987) and Labitzke and van Loon (1988), the dependence of the stability of the vortex and the temperatures in the lower polar stratosphere is more obvious during solar minimum conditions. The declining phase of solar cycle 23 was characterized by an unusually extended solar minimum lasting from 2005–2009, and even in 2004 solar activity proxies show that solar activity was already quite low. Therefore, the alternating pattern of cold and warm Arctic winters observed in Fig. 14 mainly coincides with solar minimum conditions, making the QBO signature consistent with the works by, e.g., Labitzke (1987), Labitzke and van Loon (1988) and Camp and Tung (2007).

7 Conclusions

In this study the polar vortex average technique was used for estimating ozone loss due to catalytic ozone destruction in the Arctic and Antarctic polar vortices using SCIAMACHY ozone profile observations between 2002 and 2009. The deduced polar ozone losses showed distinct interhemispheric differences. The losses in the Arctic polar vortex varied strongly from year to year, while the losses inside the Antarctic vortex were similar every year, even in the anomalous year 2002 characterized by the unusually early major stratospheric warming causing the well-documented split vortex.

ACPD
11, 6555–6599, 2011

Large ozone losses in the Arctic lower stratosphere were only found to occur during the cold winters 2004/2005 and 2006/2007. The longest depletion period occurred in the 2006/2007 winter. The highest seasonally averaged depletion rate at the 475 K isentropic level of more than 20 ppbv per day occurred in the 2004/2005 winter, corresponding to a total relative ozone loss of about 40% during the studied period. Significant depletions around 1.4–2 ppmv w ere detected in the lower stratosphere between the 450 K and 525 K isentropic levels in March 2005 and March 2007. The estimated total ozone mass loss inside the Arctic polar vortex between the 450 K and 600 K isentropic levels is about 30 million tons for the winter 2004/2005. Much lower ozone mass losses were determined for the warm winters 2002/2003, 2003/2004, 2005/2006 and 2008/2009.

Large ozone losses inside the Antarctic polar vortex were found every year with similar seasonally averaged ozone loss rates of about 28–30 ppbv per day at the 475 K level. The daily loss rates were large from August to early October, and then decreased slowly until mid-November. By that time a total relative ozone loss of about 80% or 2.5–3 ppmv inside the polar vortex at the 475 K level occurred regularly each season. The total ozone mass loss is about 55–75 million tons inside the Antarctic polar vortex between the 450 K and 600 K isentropic levels. We note, that due to the limited vertical resolution of the SCIAMACHY ozone profiles of about 4.5 km, the actual chemical ozone loss at the 475 K isentropic level may be larger. The larger ozone losses observed in the Antarctic winter stratosphere are consistent with low temperatures dominating the polar vortex over a longer period and with higher stability as compared to the Arctic stratosphere.

The vertical variation of the chemical ozone loss determined from SCIAMACHY limb observations using the vortex average method for the 2004/2005 Northern Hemisphere winter was shown to be in good agreement with the results of other instruments and techniques. The inter-annual variability in PSC occurrence rate and chemical ozone losses in the Arctic polar vortex is consistent with the known statistical dependence of vortex stability on the phase of the QBO for solar minimum conditions.

ACPD
11, 6555–6599, 2011

Acknowledgements. This work was supported by the German Ministry of Education and Research (BMBF), the German aerospace center (DLR), the University of Bremen, Germany. SCIAMACHY is jointly funded by Germany, the Netherlands and Belgium. T. S. would like to thank Lampang Rajabhat University, Thailand, for the funding support.

References

Baldwin, M. P., Gray, L. J., Dunkerton, T. J., Hamilton, K., Haynes, P. H., Randel, W. J., Holton, J. R., Alexander, M. J., Hirota, I., Horinouchi, T., Jones, D. B. A., Kinnersley, J. S., Marquardt, C., Sato, K., and Takahashi, M. : The quasibiennial oscillation, Rev. Geophys., 39, 179–229, 2001. 6574

Baldwin, M., P., Hirooka, T., O'Neil, A., and Yoden, S.: Major stratospheric warming in the southern hemisphere in 2002: Dynamical aspects of the ozone hole split, SPARC newsletter, No. 20, SPARC Office, Toronto, ON, Canada, 24–26, 2003. 6563

Becker, G., Müller, R., McKenna, D. S., Rex, M., Carslaw, K., and Oelhaf, H.: Ozone loss rates in the Arctic stratosphere in the winter 1994/1995: Model simulations underestimate results of the Match analysis, J. Geophys. Res., 105, 15175–15184, 2000. 6557

Bodeker, G. E., Shiona, H., and Eskes, H.: Indicators of Antarctic ozone depletion, Atmos. Chem. Phys., 5, 2603–2615, doi:10.5194/acp-5-2603-2005, 2005. 6563

Bovensmann, H., Burrows, J. P., Buchwitz, M., Frerick, J., Noël, S., Rozanov, V. V., Chance, K. V., and Goede, A. P. H.: SCIAMACHY: Mission objectives and measurement modes, J. Atmos. Sci., 56(2), 127–150, 1999. 6559

Braathen, G. O., Rummkainen, M., Kyrö, E., Schmidt, U., Dahlback, A., Jorgensen, T. S., Fabian, R., Rudagov, V. V., Gil, M., and Borchers, R.: Temporal development of ozone within the Arctic vortex during the winter of 1991/1992, Geophys. Res. Lett., 21, 1407–1410, 1994. 6564

Brewer, A. W.: Evidence for a world circulation provided by the measurements of helium and water vapour distribution in the stratosphere, Q. J. Roy. Meteor. Soc., 75, 351–363, doi:10.1002/qj.49707532603, 1949. 6558

Camp, C. D. and Tung, K.-K.: The influence of the solar cycle and QBO on the late-winter stratospheric polar vortex, J. Atmos. Sci, 64, 1267–1283, 2007. 6574

ACPD

11, 6555–6599, 2011

Chipperfield, M. P., Lee, A. M., and Pyle, J. A.: Model calculations of ozone depletion in the Arctic polar vortex for 1991/92 to 1994/95, Geophys. Res. Lett., 23, 559–562, 1996. 6557
National Weather Service, Climate Prediction Center: Stratosphere: Global temperature time series, available at: http://www.cpc.noaa.gov/products/stratosphere/temperature/, 2009. 6562
Deniel, C., Bevilaqua, R. M., Pommereau, J. P., and Lefèvre, F.: Arctic chemical ozone depletion during the 1994/1995 winter deduced from POAM II satellite observations and the REPROBUS three-dimensional model, J. Geophys. Res., 103, 19231–19244, 1998. 6557
Dobson, G. M. B., Kimball, H. H., and Kidson, E.: Observations of the amount of ozone in the Earth's atmosphere, and its relation to other geophysical conditions. Part IV, Proc. R. Soc. Lond. A, 129, 411–433, 1930. 6558
Dufour, G., Nassar, R., Boone, C. D., Skelton, R., Walker, K. A., Bernath, P. F., Rinsland, C. P., Semeniuk, K., Jin, J. J., McConnell, J. C., and Manney, G. L.: Partitioning between the inorganic chlorine reservoirs HCl and ClONO2 during the Arctic winter 2005 from the ACE-FTS, Atmos. Chem. Phys., 6, 2355–2366, doi:10.5194/acp-6-2355-2006, 2006. 6567, 6571
Eichmann, K.-U., Weber, M., Bramstedt, K., and Burrows, J. P.: Ozone depletion in the NH winter/spring 1999/ 2000 as measured by GOME on ERS-2, J. Geophys. Res., 107, 8280, doi:10.1029/2001JD001148, 2002. 6557, 6561, 6564
EU: European research in the stratosphere 1996-2000, chap. 3.5, 112–117, EUR 19867, Brussels, 2001. 6557
Farman, J. C., Gardiner, B. G., and Shanklin, J. D.: Large losses of total ozone in Antarctica reveal seasonal ClOx/NOx interaction, Nature, 315, 207–210, 1985. 6557
Fussen, D. and López-Puertas, M: Summary on upper atmosphere, Atmospheric Science Conference, Barcelona, Spain, 7–11 September, 2009. 6562
Goutail, F., Harris, N. R. P., Kilbane-Dawe, I., and Amanatidis, G. T.: Ozone loss: the global picture, Proc. European Ozone Meeting, Schliersee, Germany, 1997. 6557
Goutail, F., Pommereau, J.-P., Lefèvre, F., van Roozendael, M., Andersen, S. B., Kåstad Høiskar, B.-A., Dorokhov, V., Kyrö, E., Chipperfield, M. P., and Feng, W.: Early unusual ozone loss during the Arctic winter 2002/2003 compared to other winters, Atmos. Chem. Phys., 5, 665–677, doi:10.5194/acp-5-665-2005, 2005. 6557
Grooß, J.-U. and Müller, R.: The impact of mid-latitude intrusions into the polar vortex on ozone loss estimates, Atmos. Chem. Phys., 3, 395–402, doi:10.5194/acp-3-395-2003, 2003. 6557
Grooß, J.-U., Günther, G., Müller, R., Konopka, P., Bausch, S., Schlager, H., Voigt, C., Volk,

ACPD
11, 6555–6599, 2011

C. M., and Toon, G. C.: Simulation of denitrification and ozone loss for the Arctic winter 2002/2003, Atmos. Chem. Phys., 5, 1437–1448, doi:10.5194/acp-5-1437-2005, 2005. 6567
Grooß, J.-U. and Müller, R.: Simulation of ozone loss in Arctic winter 2004/2005, Geophys. Res. Lett., 34, L05804, doi:10.1029/2006GL028901, 2007. 6567, 6571, 6572, 6573, 6597
Grooß, J.-U., Müller, R., Konopka, P., Steinhorst, H.-M., Engel, A., Möbius, T., and Volk, C. M.: The impact of transport across the polar vortex edge on Match ozone loss estimates, Atmos. Chem. Phys., 8, 565–578, doi:10.5194/acp-8-565-2008, 2008. 6572
Guirlet, M., Chipperfield, M. P., Pyle, J. A., Goutail, F., Pommereau, J. P., and Kyrö, E.: Modeled Arctic ozone depletion in winter 1997/1998 and comparison with previous winters, J. Geophys. Res., 105, 22185–22200, 2000. 6557
Harris, N. R. P., Rex, M., Goutail, F., Knudsen, B. M., Manney, G. L., Müller, R., and von der Gathen, P.: Comparison of empirically derived ozone losses in the Arctic vortex, J. Geophys. Res., 107(D20), 8264, doi:10.1029/2001JD000482, 2002. 6557
Haynes, P. H., Marks, C. J., McIntyre, M. E., Shepherd, T. G., and Shine, K. P.: On the "downward control" of extratropical diabatic circulations by eddy-induced mean zonal forces, J. Atmos. Sci., 48, 651–678, 1991. 6558
Holton, J. R. and Tan, H. C.: The influence of the equatorial QBO in the global circulation at 50mb, J. Atmos. Sci., 37, 2200–2208, 1980. 6574
Holton J. R., Haynes, P. H., McIntyre, M. E., Douglass, A. R., Rood, R. B., and Pfister, L.: Stratosphere-troposphere exchange, Rev. Geophys., 33, 403–439, 1995. 6558
Holton, J. R. and Alexander, M. J.: The role of waves in the transport circulation of the middle atmosphere, in: Atmospheric Sciences Across the Stratopause, edited by: Siskind, D. E., Eckermann, S. D., and Summers, M. E., Geophysical Monograph Series No. 123, AGU, 21–35, 2000. 6562
Hoogen, R., Rozanov, V. V., and Burrows, J. P.: Ozone profiles from GOME satellite data: Algorithm description and first validation, J. Geophys. Res., 104, 8263–8280, 1999. 6564
Hoppel, K., Bevilacqua, R., Allen, D., Nedoluha, G., and Randall C.: POAM III observations of the anomalous 2002 Antarctic ozone hole, Geophys. Res. Lett., 30(7), 1394, doi:10.1029/2003GL016899, 2003. 6557, 6563, 6569, 6570
IPCC/TEAP: Special report on safeguarding the ozone layer and the global climate system, Cambridge University Press, Cambridge, United Kingdom, New York, USA, 2005. 6563
Jones, A., Urban, J., Murtagh, D. P., Eriksson, P., Brohede, S., Haley, C., Degenstein, D., Bourassa, A., von Savigny, C., Sonkaew, T., Rozanov, A., Bovensmann, H., and Burrows,

ACPD
11, 6555–6599, 2011

J.: Evolution of stratospheric ozone and water vapour time series studied with satellite measurements, Atmos. Chem. Phys., 9, 6055–6075, doi:10.5194/acp-9-6055-2009, 2009. 6557, 6560

Jucks, K. W. and Salawitch, R. J.: Future changes in upper stratospheric ozone, in: atmospheric science across the stratopause, edited by: Siskind, D. E., Eckermann, S. D., and Summers, M. E., Geophys. Mono., 123, AGU, 241–255, 2000. 6558

Knudsen, B. M., Larsen, N., Mikkelsen, I. S., Morcrette, J.-J., Braathen, G. O., Kyrö, E., Fast, H., Gernandt, H., Kanzawa, H., Nakane, H., Dorokhov, V., Yushkov, V., Hansen, G., Gil, M., and Shearman, R. J.: Ozone depletion in and below the Arctic vortex for 1997, Geophys. Res. Lett., 25, 627–630, 1998. 6557

Konopka, P., Grooß, J.-U., Hoppel, K. W., Steinhorst, H.-M., and Müller, R.: Mixing and chemical ozone loss during and after the Antarctic polar vortex major warming in September 2002, J. Atmos. Sci., 62, 848–859, doi:10.1175/JAS-3329.1, 2005. 6563

Konopka, P., Engel, A., Funke, B., Müller, R., Grooß, J.-U., Günther, G., Wetter, T., Stiller, G., von Clarmann, T., Glatthor, N., Oelhaf, H., Wetzel, G., López-Puertas, M., Pirre, M., Huret, N., and Riese, M.: Ozone loss driven by nitrogen oxides and triggered by stratospheric warmings can outweigh the effect of halogens, J. Geophys. Res., 112, D5105, doi:10.1029/2006JD007064, 2007. 6567

Kushner, P. L. and Polvani, L. M.: A very large, spontaneous stratospheric sudden warming in a simple AGCM: A prototype for the southern hemisphere warming of 2002?, J. Atmos. Sci., 62, 890–897, 2004. 6563

Labitzke, K.: Sunspots, the QBO, and the stratospheric temperature in the north polar-region, Geophys. Res. Lett., 14, 535–537, 1987. 6574

Labitzke, K. and van Loon, H.: Associations between the 11-year solar-cycle, the QBO and the atmosphere. Part I: The troposphere and stratosphere in the northern hemisphere in winter, J. Atmos. Terr. Phys., 50, 197–206, 1988. 6574

Lait, L. R.: An alternative form for potential vorticity, J. Atmos. Sci., 51, 1754–1759, 1994. 6561

Manney, G. L., Krüger, K., Sabutis, J. L., Sena, S. A., and Pawson, S.: The remarkable 2003–2004 and other recent warm winter in the Arctic stratosphere since the late 1990s, J. Geophys. Res., 110, D04107, doi:10.1029/2004JD005367, 2005a. 6562, 6565

Manney, G. L., Sabutis, J. L., Allen, D. R., Lahoz, W. A., Scaife, A. A., Randall, C. E., Pawson, S., Naujokat, B., and Swinbank, R.: Simulations of dynamics and transport during the September 2002 Antarctic major warming, J. Geophys. Res., 62, 690–707, doi:10.1175/JAS-

ACPD
11, 6555–6599, 2011

3313.1, 2005b. 6563
Manney, G. L., Schwartz, M. J., Krüger, K., Santee, M. L., Pawson, S., Lee, J. N., Daffer, W. H., Fuller, R. A., and Livesey, J.: Aura Microwave Limb Sounder Observations of dynamics and transport during the record-breaking 2009 Arctic stratospheric major warming, Geophys. Res. Lett., 36, L12815, doi:10.1029/2009GL038586, 2009. 6562
Nash, E. R., Newman, P. A., Rosenfield, J .E., and Schoeberl, M. R.: An objective determination of the polar vortex using Ertels potential vorticity, J. Geophys. Res., 101(D5), 9471-9478, 1996. 6561
Newchurch, M. J., Yang, E.-S., Cunnold, D. M., Reinsel, G. C., Zawodny, J. M., and Russell III, J. M.: Evidence for slowdown in stratospheric ozone loss: First stage of ozone recovery, J. Geophys. Res., 108, 4507, doi:10.1029/2003JD003471, 2003. 6557
Newman, P. A. and Nash, E. R.: The unusual southern hemisphere stratosphere winter of 2002, J. Atmos. Sci., 62, 614–628, 2005. 6563
Randel, W. J., Wu, F., Russell III, J. M., Roche, A., and Waters, J. W.: Seasonal cycles and QBO variations in stratospheric CH_4 and H_2O observed in UARS HALOE data, J. Atmos. Sci., 55, 163–185, 1998. 6564
Remsberg, E. E., Marshall, B. T., Garcia-Comas, M., Krueger, D., Lingenfelser, G. S., Martin-Torres, J., Mlynczak, M. G., Russell, J. M., Smith, A. K., Zhao, Y., Brown, C., Gordley, L. L., Lopez-Gonzalez, M. J., Lopez-Puertas, M., She, C.-Y., Taylor, M. J., and Thompson, R. E.: Assessment of the quality of the Version 1.07 temperature-versus-pressure profiles of the middle atmosphere from TIMED/SABER, J. Geophys. Res.-Atmos., 113, D17101, doi:10.1029/2008JD010013, 2008. 6562
Rex, M., von der Gathen, P., Braathen, G. O., Harris, N. R. P., Reimer, E., Beck, A., Alfier, R., Krüger-Carstensen, R., Chipperfield, M., De Backer, H., Balis, D., O'Connor, F., Dier, H., Dorokhov, V., Fast, H., Gamma, A., Gil, M., Kyrö, E., Litynska, Z., Mikkelsen, I. S., Molyneux, M., Murphy, G., Reid, S. J., Rummukainen, M., and Zerefos, D.: Chemical ozone loss in the Arctic winter 1994/1995 as determined by the Match technique, J. Atmos. Chem., 32, 35–59, 1999. 6557
Rex, M., Salawitch, R. J., Harris, N. R. P., von der Gathen, P., Braathen, G. O., Schulz, A., Deckelmann, H., Chipperfield, M., Sinnhuber, B.-M., Reimer, E., Alfier, R., Bevilacqua, R., Hoppel, K., Fromm, M., Lumpe, J., Küllmann, H., Kleinböhl, A., Bremer, H., von König, M., Künzi, K., Toohey, D., Vömel, H., Richard, E., Aikin, K., Jost, H., Greenblatt, J. B., Loewenstein, M., Podolske, J. R., Webster, C. R., Flesch, G. J., Scott, D. C., Herman, R.

ACPD
11, 6555–6599, 2011

L., Elkins, J. W., Ray, E. A., Moore, F. L., Hurst, D. F., Romashkin, P., Toon, G. C., Sen, B., Margitan, J. J., Wennberg, P., Neuber, R., Allart, M., Bojkov, B. R., Claude, H., Davies, J., Davies, W., De Backer, H., Dier, H., Dorokhov, V., Fast, H., Kondo, Y., Kyrö, E., Litynska, Z., Mikkelsen, I. S., Molyneux, M. J., Moran, E., Nagai, T., Nakane, H., Parrondo, C., Ravegnani, F., Skrivankova, P., Viatte, P., and Yushkov, V.: Chemical depletion of Arctic ozone in winter 1999/2000, J. Geophys. Res., 107(D20), 8276, doi:10.1029/2001JD000533, 2002. 6557

Rex, M., Salawitch, R. J., Santee, M. L., Waters, J. W., Hoppel, K., and Bevilaqua, R.: On the unexplained stratospheric ozone losses during cold Arctic Januaries, Geophys. Res. Lett., 30(1), 1008, doi:10.1029/2002GL016008, 2003. 6557

Rex, M., Salawitch, R. J., Deckelmann, H., von der Gathen, P., Harris, N. R. P., Chipperfield, M. P., Naujokat, B., Reimer, E., Allaart, M., Andersen, S. B., Bevilacqua, R., Braathen, G. O., Claude, H., Davies, J., De Backer, H., Dier, H., Dorokhov, V., Fast, H., Gerding, M., Godin-Beekmann, S., Hoppel, K., Johnson, B., Kyrö, E., Litynska, Z., Moore, D., Nakane, H., Parrondo, M. C., Risley, A. D., Skrivankova, P., Stübi, R., Viatte, P., Yushkov, V., and Zerefos, C.: Arctic winter 2005: Implications for stratospheric ozone loss and climate change, Geophys. Res. Lett., 33, L23808, doi:10.1029/2006GL026731, 2006. 6571, 6572, 6573, 6597

Ricaud, P., Lefèvre, F., Berthet, G., Murtagh, D., Llewellyn, E. J., Mégie, G., Kyrölä, E., Leppelmeier, G. W., Auvinen, H., Boone, C., Brohede, S., Degenstein, D. A., de La Noë, J., Dupuy, E., El Amraoui, L., Eriksson, P., Evans, W. F. J., Frisk, U., Gattinger, R. L., Girod, F., Haley, C. S., Hassinen, S., Hauchecorne, A., Jimenez, C., Kyrö, E., Lautié, N., Le Flochmoën, E., Lloyd, N. D., McConnell, J. C., McDade, I. C., Nordh, L., Olberg, M., Pazmino, A., Petelina, S. V., Sandqvist, A., Seppälä, A., Sioris, C. E., Solheim, B. H., Stegman, J., Strong, K., Taalas, P. Urban, J., von Savigny, C., von Scheele, F., and Witt, G.: Polar vortex evolution during the 2002 Antarctic major warming as observed by the Odin satellite, J. Geophys. Res., 110(9), D05302, doi:10.1029/2004JD005018, 2005. 6563

Rosenlof, K. H.: Seasonal cycle of the residual mean meridional circulation in the stratosphere, J. Geophys. Res., 100, 5173–5191, 1995. 6558

Rösevall, J. D., Murtagh, D. P., Urban, J., Feng, W., Eriksson, P., and Brohede, S.: A study of ozone depletion in the 2004/2005 Arctic winter based on data from Odin/SMR and Aura/MLS, J. Geophys. Res., 113, D13301, doi:10.1029/2007JD009560, 2008. 6571

Rozanov, A., Rozanov, V., Buchwitz, M., Kokhanovsky, A., and Burrows, J. P.: SCIATRAN 2.0 – A new radiative transfer model for geophysical applications in the 175–2400 nm spectral

ACPD
11, 6555–6599, 2011

region, Adv. Space Res., 36, 1015–1019, 2005. 6560
Rozanov, A.: SCIATRAN 2.X: Radiative transfer model and retrieval software package, available at: http://www.iup.physik.uni-bremen.de/sciatran, 2008. 6560
Sathishkumar, S., Sridharan, S., and Jocobi, Ch.: Dynamical response of low-latitude middle atmosphere to major sudden stratospheric warming events, J. Atmos. Sol.-Terr. Phys., 71, 857–865, 2009. 6562
Shine, K. P.: On the cause of the relative greenhouse strength of gases such as the halocarbons, J. Atmos. Sci., 48, 1513–1518, 1991. 6564
Singleton, C. S., Randall, C. E., Chipperfield, M. P., Davies, S., Feng, W., Bevilacqua, R. M., Hoppel, K. W., Fromm, M. D., Manney, G. L., and Harvey, V. L.: 2002–2003 Arctic ozone loss deduced from POAM III satellite observations and the SLIMCAT chemical transport model, Atmos. Chem. Phys., 5, 597–609, doi:10.5194/acp-5-597-2005, 2005. 6557, 6571
Singleton, C. S., Randall, C. E., Harvey, V. L., Chipperfield, M. P., Feng, W., Manney, G. L., Froidevaux, L., Boone, C. D., Bernath, P. F., Walker, K. A., McElroy, C. T. and Hoppel, K. W.: Quantifying Arctic ozone loss during the 2004-2005 winter using satellite observations and a chemical transport model, J. Geophys. Res.-Atmos., 112, D7304, doi:10.1029/2006JD007463, 2007. 6571, 6572, 6573
Siskind, D. E., Froidevaux, L., Russell, J. M., and Lean, J.: Implications of upper stratospheric trace constituent changes observed by HALOE for O_3 and ClO from 1992 to 1995, Geophys. Res. Lett., 25(18), 3513–3516, 1998. 6558
Solomon, S.: Stratospheric ozone depletion: A review of concepts and history, Rev. Geophys., 37, 275–316, 1999. 6557, 6558, 6567
Solomon S., Portmann, R. W., Sasaki, T., Hofmann, D. J., and Thompson, D. W. J.: Four decades of ozonesonde measurements over Antarctica, J. Geophys. Res., 110, D21311, doi:10.1029/2005JD005917, 2005. 6557
Solomon, S., Portmann, R. W., and Thompson, D. W. J.: Contrasts between Antarctic and Arctic ozone depletion, P. Natl. Acad. Sci., 104(2), 445–449, 2007. 6557
Sonkaew, T., Rozanov, V. V., von Savigny, C., Rozanov, A., Bovensmann, H., and Burrows, J. P.: Cloud sensitivity studies for stratospheric and lower mesospheric ozone profile retrievals from measurements of limb-scattered solar radiation, Atmos. Meas. Tech., 2, 653–678, doi:10.5194/amt-2-653-2009, 2009. 6560
Steinbrecht, W., Claude, H., Schönenborn, F., McDermid, I. S., Leblanc, T., Godin, S., Keckhut, P., van Gijsel, A., Swart, D. P. J., Bodeker, G., Parrish, A., Boyd, I., Kämpfer, N., Hocke, C.,

ACPD
11, 6555–6599, 2011

Stolarski, R. S., Frith, S. M., Thomason, L. W., Remsberg, E. E., von Savigny, C., Rozanov, A., and Burrows, J. P.: Ozone and temperature trends in the upper stratosphere at five stations of the Network for the Detection of Atmospheric Composition Change, Int. J. Remote Sens., 30(15–16), 3875–3886, 2009. 6557, 6560

Stolarski, R. S., McPeters, R. D., and Newman, P. A.: The ozone hole of 2002 as measured by TOMS, J. Atmos. Sci., 62(3), 716–720, 2005. 6563

Swinbank, R. and O'Neill, A.: A stratosphere-troposphere data assimilation system, Mon. Weather Rev., 122, 686–702, 1994. 6560

von Savigny, C., Rozanov, A., Bovensmann, H., Eichmann, K.-U., Noël, S., Rozanov, V., Sinnhuber, B.-M., Weber, M., Burrows, J. P., and Kaiser, J. W.: The ozone hole breakup in September 2002 as seen by SCIAMACHY on ENVISAT, J. Atmos. Sci., 62(3), 721–734, 2005a. 6560, 6563, 6570, 6571

von Savigny, C., Ulasi, E. P., Eichmann, K.-U., Bovensmann, H., and Burrows, J. P.: Detection and mapping of polar stratospheric clouds using limb scattering observations, Atmos. Chem. Phys., 5, 3071–3079, doi:10.5194/acp-5-3071-2005, 2005b. 6560, 6561

Weber, M., Dhomse, S., Wittrock, F., Richter, A., Sinnhuber, B.-M., and Burrows, J. P.: Dynamical control of NH and SH winter/spring total ozone from GOME observations in 1995–2002, Geophys. Res. Lett., 30(11), 1583, doi:10.1029/2002GL016799, 2003. 6558, 6569

ACPD
11, 6555–6599, 2011

Table 1. The chemical ozone loss rates in the Arctic polar vortex between 450 K and 600 K isentropic levels for the winters 2002/2003 to 2008/2009.

Year	Studied period		Chemical O_3 loss (ppbv day^{-1})							
	Start day	End day	average[1]	linear fit[2]						
			475 K	450 K	475 K	500 K	525 K	550 K	575 K	600 K
2003	13	106	−6.9	−8.4	−4.5	−0.02	+1.7	−0.07	−4.8	−13.1
2004	8	106	−4.6	+7.8	+1.9	+4.3	+6.9	+3.8	−3.9	−12.3
2005	20	92	−26.1	−24.5	−23.2	−15.2	−11.0	−9.0	−12.7	−18.3
2007	17	119	−20.1	−16.2	+15.0	−13.4	−11.1	−11.3	−14.1	−18.0
2008	7	96	−11.3	−12.2	−13.6	−11.5	−10.0	−11.4	−15.3	−19.3
2006	14	51	+11.1	−10.2	−14.2	+14.7	+17.4	+7.3	−4.7	−14.3
2009	26	46	−44.9	−49.9	−35.6	−19.3	−1.9	−25.6	−35.7	−36.1

[1] average for period studied at 475 K isentropic level,
[2] from linear fit (e.g., dashed line in Fig. 3d for the 475 K isentropic level).
Shown separately at the bottom of table is for seasons when short periods of polar vortex are observed.

ACPD
11, 6555–6599, 2011

Table 2. The chemical ozone loss rates in the Antarctic polar vortex between 450 K and 600 K isentropic levels between 15 August and 15 November of the years 2002–2008.

Year	Chemical O_3 loss (ppbv day^{-1})							
	average[1]	linear fit[2]						
	475 K	450 K	475 K	500 K	525 K	550 K	575 K	600 K
2002	−32.4	−24.7	−29.0	−31.3	−34.4	−38.4	−36.9	−35.9
2003	−28.1	−23.8	−27.7	−28.6	−28.4	−28.2	−29.1	−28.4
2004	−28.6	−26.1	−29.3	−30.3	−29.2	−27.3	−25.9	−25.2
2005	−29.0	−23.8	−26.2	−25.0	−24.2	−24.5	−26.3	−27.2
2006	−28.2	−25.3	−28.5	−31.6	−30.4	−27.7	−23.2	−20.1
2007	−32.9	−25.4	−31.4	−35.3	−33.4	−32.4	−31.1	−30.1
2008	−29.4	−25.6	−30.0	−31.9	−30.1	−26.4	−27.0	−23.9

[1] average for period from 15 August to 15 November,

[2] from linear fit (e.g., dashed line in Fig. 8d).

ACPD
11, 6555–6599, 2011

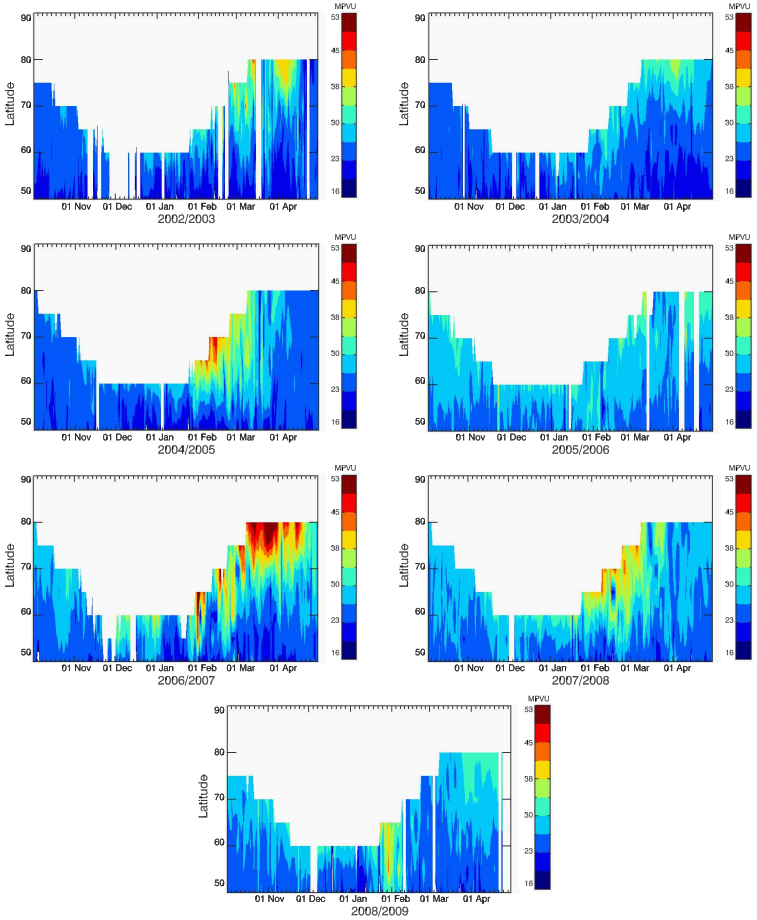

Fig. 1. Daily and zonally averaged modified potential vorticity at the 475 K isentropic level in the Arctic stratosphere for latitudes of SCIAMACHY observations in 2002–2009 during winter/spring (given in modified potential vorticity units (MPVU)). Data averaged over 5° latitude bins.

ACPD
11, 6555–6599, 2011

Chemical ozone loss from limb SCIAMACHY

T. Sonkaew et al.

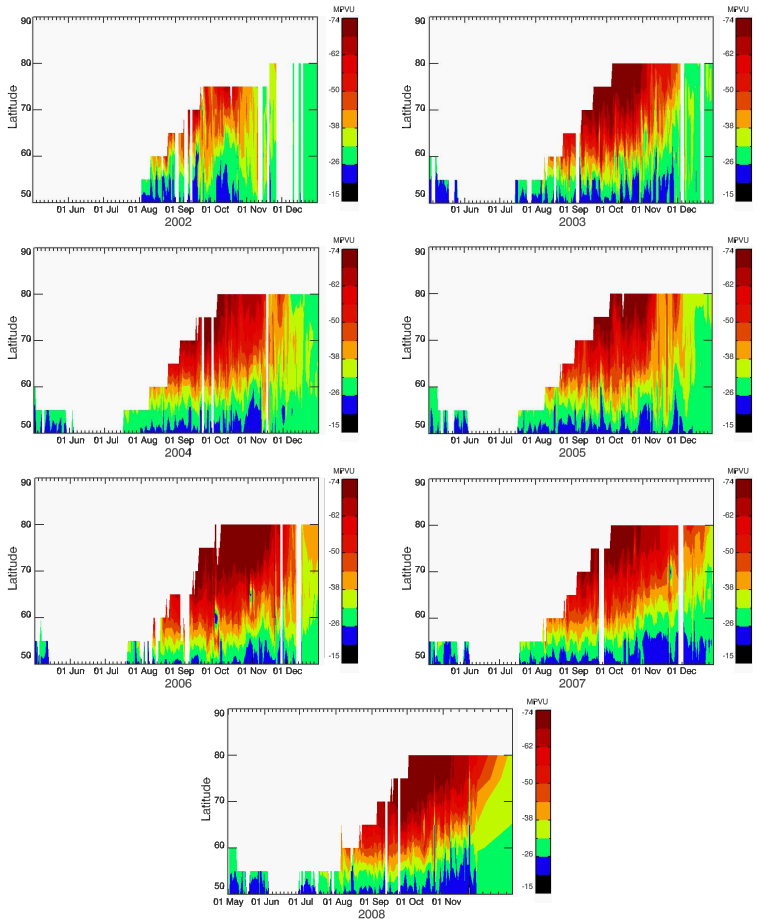

Fig. 2. Daily and zonally averaged modified potential vorticity at the 475 K isentropic level in the Antarctic stratosphere for the latitudes of SCIAMACHY observations in 2002–2008 during winter/spring.

ACPD
11, 6555–6599, 2011

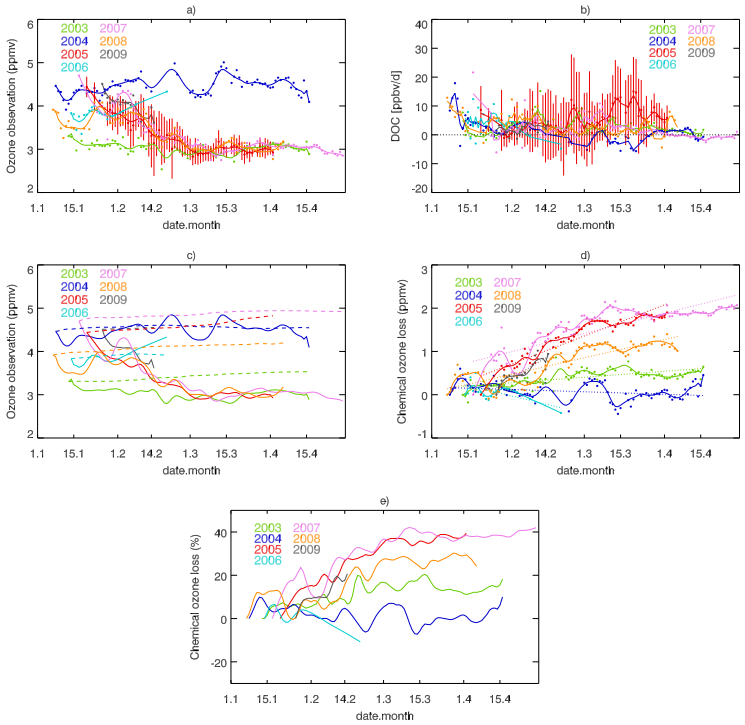

Fig. 3. Chemical ozone loss results for the Arctic polar vortices 2002/2003 to 2008/2009 at the 475 isentropic level. **(a)** Observed vortex average ozone mixing ratio time series. **(b)** Daily change in ozone mixing ratio due to diabatic descent determined with MIDRAD model simulations. **(c)** Accumulated ozone mixing ratio from daily diabatic descent (dashed lines) and the observed ozone mixing ratio time series (solid lines). **(d)** Chemical ozone losses in ppmv (solid lines) and linear fits to the chemical ozone losses (dashed lines). **(e)** Chemical ozone loss in percent relative to the start days listed in Table 1.

ACPD
11, 6555–6599, 2011

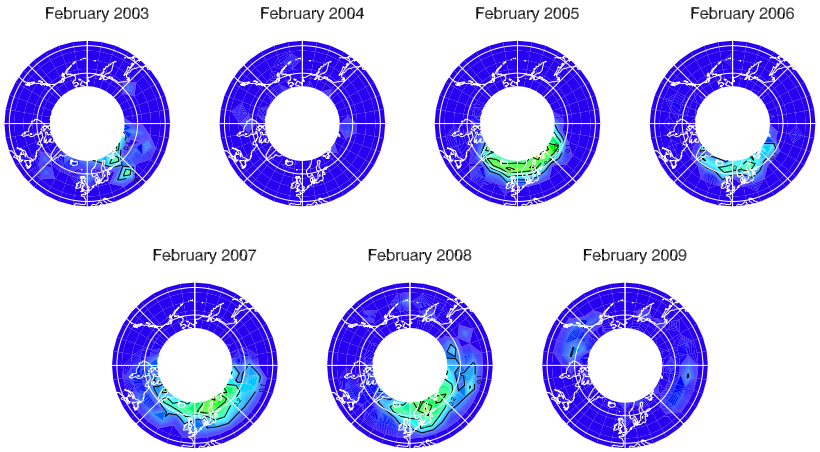

Fig. 4. Maps of PSC occurrence rates in the northern polar atmosphere for February of the years 2003–2009. Contour levels are 0.1, 0.2 and 0.3.

ACPD
11, 6555–6599, 2011

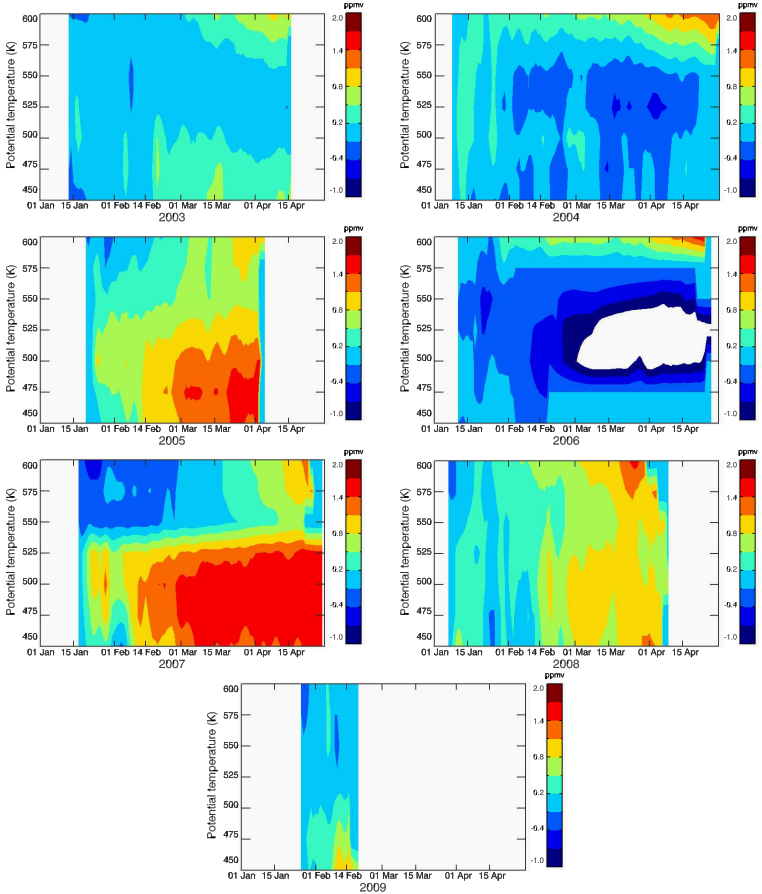

Fig. 5. Derived vortex average ozone losses as a function of time and potential temperature for the years 2003 to 2009 in the Arctic winter stratosphere.

ACPD
11, 6555–6599, 2011

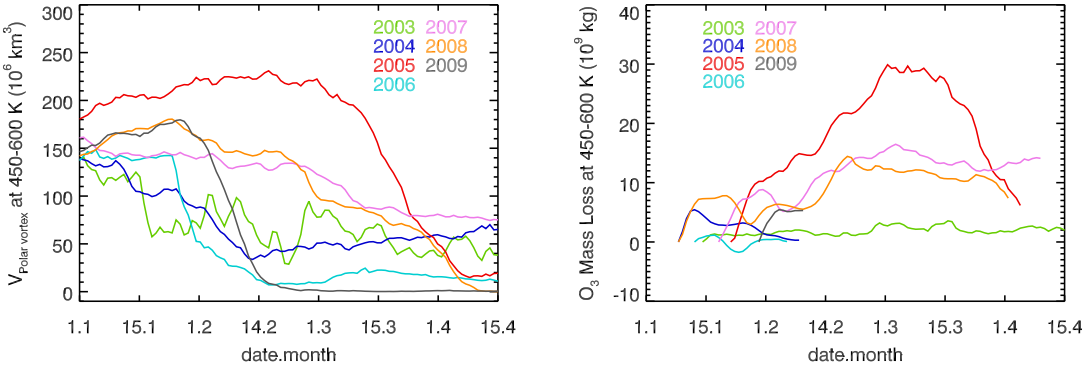

Fig. 6. Time evolution of the polar vortex volume (left panel), and the estimated ozone mass loss inside the vortex (right panel) between the 450 K and 600 K isentropic levels in the Arctic winter stratosphere.

ACPD
11, 6555–6599, 2011

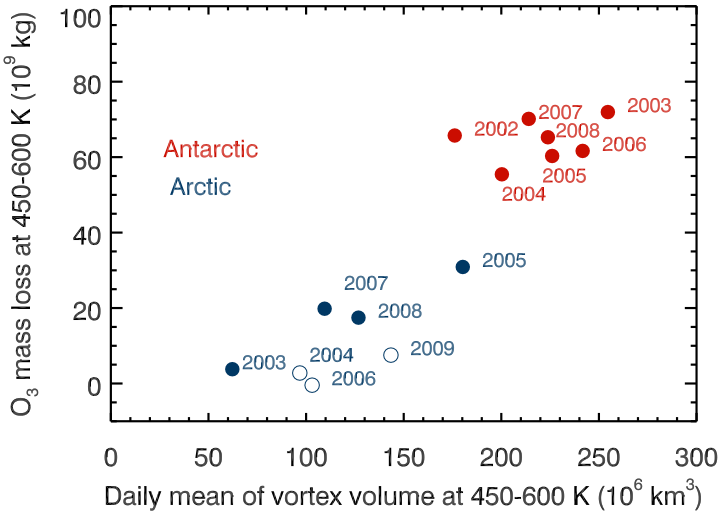

Fig. 7. Scatter plot of averaged daily polar vortex volume and ozone mass loss at potential temperatures of 450–600 K isentropic levels in the Arctic during the period times indicated in the right panel of Fig. 6 (blue) and Antarctic between 15 August and 15 November (red) winter stratospheres.

ACPD
11, 6555–6599, 2011

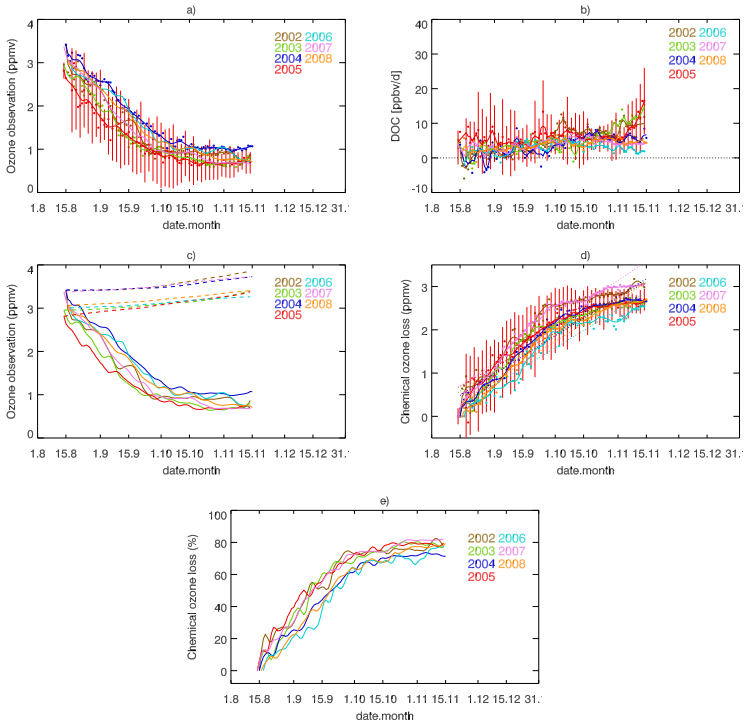

Fig. 8. Chemical ozone loss results for the Antarctic polar vortices 2002 to 2008 at the 475 isentropic level. **(a)** Observed vortex average ozone mixing ratio time series. **(b)** Daily change in ozone mixing ratio due to diabatic descent determined with MIDRAD model simulations. **(c)** Accumulated ozone mixing ratio from daily diabatic descent (dashed lines) and the observed ozone mixing ratio time series (solid lines). **(d)** Chemical ozone losses in ppmv (solid lines) and linear fits to the chemical ozone losses (dashed lines). **(e)** Chemical ozone loss in percent relative to 15 August of each year.

ACPD
11, 6555–6599, 2011

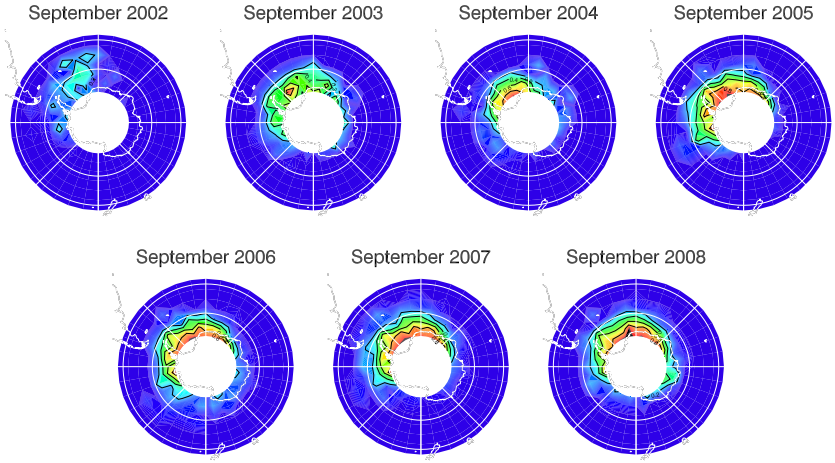

Fig. 9. Maps of PSC occurrence rates in the southern polar atmosphere for September of the years 2002–2008. Contour levels are 0.2, 0.4, 0.6 and 0.8.

ACPD
11, 6555–6599, 2011

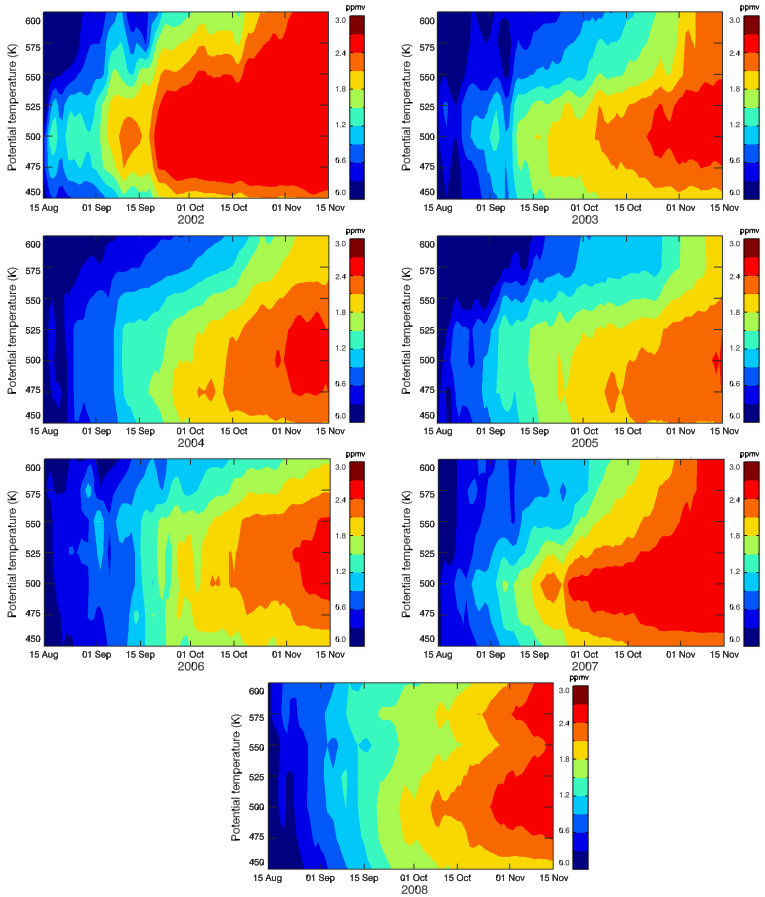

Fig. 10. Derived vortex average ozone losses as a function of time and potential temperature between the 450 K and 600 K isentropic levels in the Antarctic winter stratosphere for the years 2002 to 2008.

ACPD
11, 6555–6599, 2011

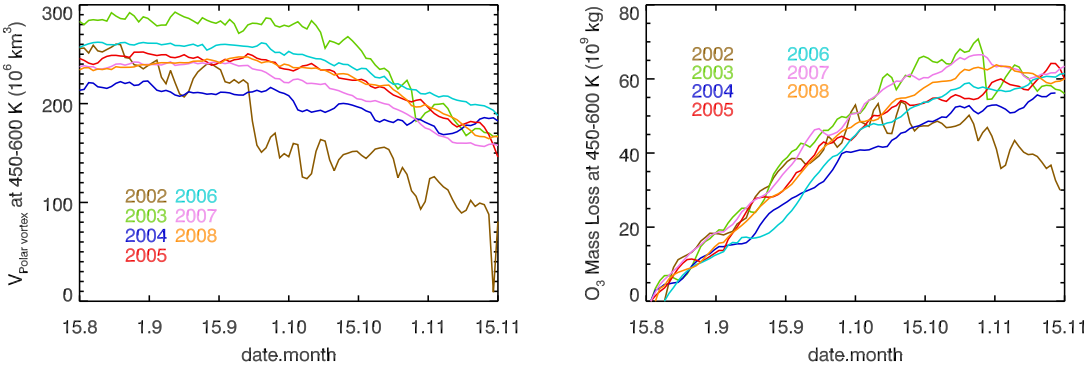

Fig. 11. Time evolution of the polar vortex volume (left panel) and the ozone mass loss inside the vortex (right panel) between the 450 K and 600 K isentropic levels in the Antarctic winter stratosphere.

ACPD
11, 6555–6599, 2011

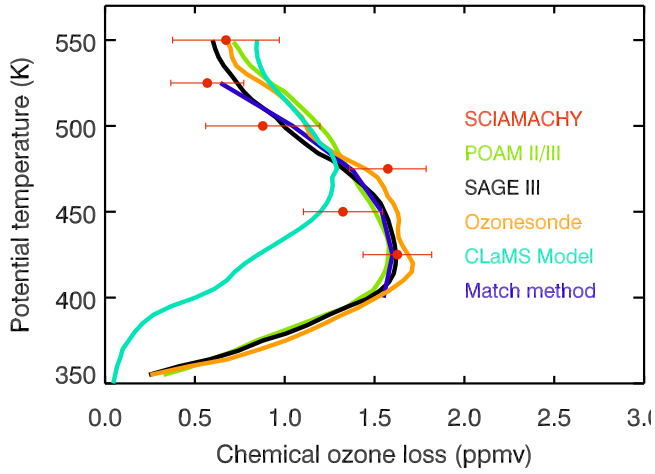

Fig. 12. Comparison of the vertical variation of the chemical ozone loss in the Arctic polar vortex for the time period 5 January–25 March 2005 estimated using various data sources and techniques. The POAM, SAGE, ozone sonde as well as the match technique data were taken from Rex et al. (2006). The CLaMS model data are based on Grooß and Müller (2007).

ACPD
11, 6555–6599, 2011

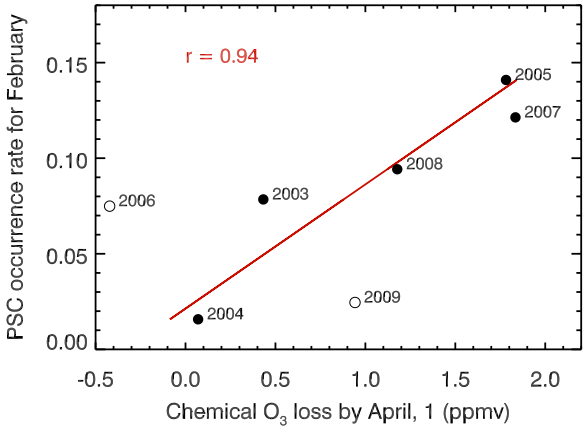

Fig. 13. Scatter plot of chemical ozone loss at the 475 K isentropic level by 1 April and the PSC occurrence rate in February for the Northern Hemisphere from SCIAMACHY limb measurements. Note, that the open circles for the years of 2006 and 2009 show the calculated chemical ozone loss up to a date well before 1 April. The solid line shows a linear fit to the data points except for the years 2006 and 2009.

ACPD
11, 6555–6599, 2011

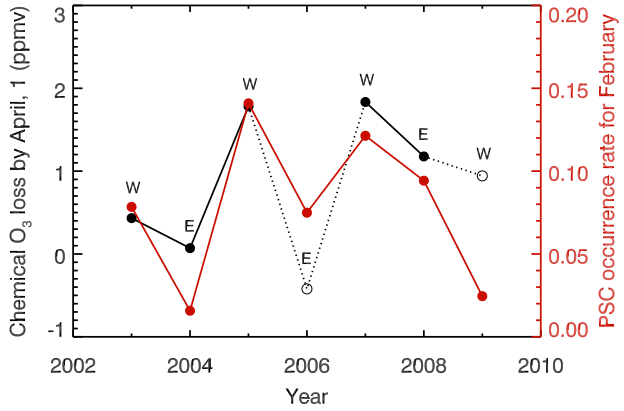

Fig. 14. Time series of accumulated chemical ozone loss at the 475 K isentropic level (until 1 April) and PSC occurrence rate for the month of February and the 40°–65° N latitude range. W and E indicate the westerly and easterly phases of the QBO. The open circles for the years 2006 and 2009 show the calculated chemical ozone loss up to a date well before 1 April.

ACPD
11, 6555–6599, 2011